Rev. Adv. Mater. Tech. vol. 3 no 2 (2021) 53–59
DOI: 10.17586/2687-0568-2021-3-2-53-59

Collective Migration of Low-Angle Tilt Boundaries Near Crack Tips in Nanocrystalline Metals Under Fatigue Load

Ya.V. Konakov and A.G. Sheinerman

Institute for Problems in Mechanical Engineering, Russian Academy of Sciences, St. Petersburg 199178, Russia

Received: May 14, 2021

Abstract. A model is suggested that describes the collective migration of two low-angle tilt boundaries near a crack tip in a nanocrystalline metal under fatigue loading. The dependences of the migration mode on the applied load and the geometric parameters of the migrating boundaries are revealed. The simulations show that the possible migration modes incorporate the reverse motion of grain boundaries (GBs), GB fragmentation, and the coalescence of low-angle GBs or their fragments with high-angle GBs. It is demonstrated that at high values of the applied load, the collective migration of the studied boundaries can lead to grain growth.

1. INTRODUCTION

In recent years, much attention has been paid to the study of nanocrystalline (NC) metallic materials, as well as to the unique physical and mechanical properties that they exhibit [1–7]. It is known that these properties significantly depend on the mechanisms of plastic deformation of such materials. For example, athermal migration of grain boundaries (GBs) under the action of an external load can lead to undesirable grain growth and, as a result, to degradation of the functional properties of NC metals [8–21].

Recently, a number of works have been devoted to the study of GB migration and grain growth in NC metallic materials (see, for example, review [22]). For example, the collective migration of low-angle GBs near the crack tip under the action of the applied stress and their complete or partial annihilation, resulting in grain growth, were revealed in experiments [21] with NC Ni-Fe alloy and molecular dynamics simulations of Au nanocrystals [23]. However, experiments [21] also observed the return of many low-angle GBs to their initial positions, which they occupied before the start of migration, after the disappearance of the external load. In our earlier work [24], a similar migration of low-angle GBs was considered, but the possible features of the influence of a crack on the described process were not taken into account. The purpose of this article is to build a model of athermal migration of two parallel low-angle GBs under the influence of a periodically acting tensile load near the crack tip and to study the characteristic dependences of this process on various system parameters.

2. MODEL

Let us consider a nanocrystalline metal consisting of grains separated by high- and low-angle grain boundaries. Let us study in more detail a group of three square grains: EABF (G1), ACDB (G2), and CGHD (G3), located near the crack tip and surrounded by high-angle GBs, separated from each other by symmetrical low-angle tilt boundaries (Fig. 1). We will consider the case in which the dislocations that make up the low-angle tilt boundaries migrate under the influence of a tensile load σ acting with a constant

Corresponding author: A.G. Sheinerman, e-mail: asheinerman@gmail.com

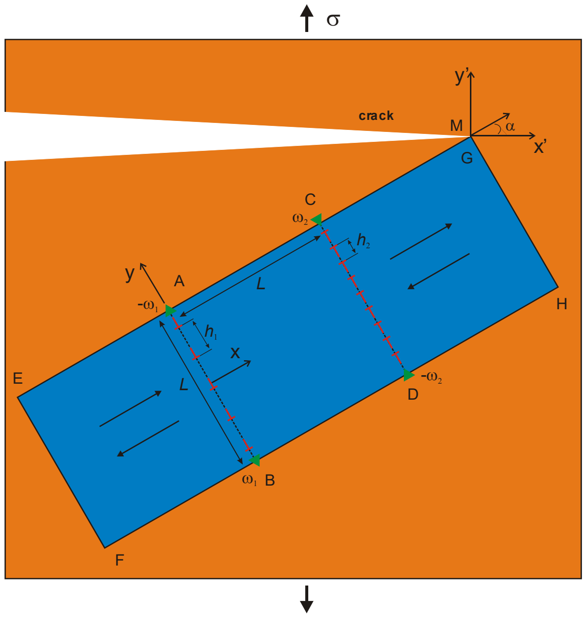

Fig. 1. Collective migration of low-angle grain boundaries under the action of an external load in a nanocrystalline metal.

duration at regular intervals. The periodic load within each loading cycle is equal to σ during some time t_1, and to zero during some time t_2.

Following [24], consider a two-dimensional model of a homogeneous metallic material. Let us denote the length of the crack as $2l$, and the position of its tip by the point M (in Fig. 1, it coincides with the point G). Within the proposed model, we will consider low-angle tilt boundaries AB (1) and CD (2) before the onset of migration as the walls of edge lattice dislocations with Burgers vectors of equal magnitude and opposite signs. The low-angle GBs are characterized by the misorientations θ_k determined by the Frank relation: $\sin(\theta_k/2) = b/(2h_k)$, $k = 1, 2$, where h_k are the periods and b is the magnitude of the Burgers vectors of the boundaries (1) and (2). We will assume that the triple junctions of grain boundaries A, B, C and D are compensated and contain wedge disclinations of strength $-\omega_1$, ω_1, ω_2 and $-\omega_2$, respectively (Fig. 1), which are related to the misorientation angles θ_1 and θ_2 of the GBs AB and CD by the relation $\omega_k = \theta_k$ $(k = 1, 2)$.

Next, we simulate the migration of GBs AB and CD under the influence of an inhomogeneous shear stress τ created by the tensile load σ directed perpendicular to the crack plane. To solve this problem, we will use the methods of two-dimensional dislocation dynamics in solids (e.g., [25–27]). For simplicity, we assume that the process under consideration occurs at low homological temperatures and there are no effects associated with thermally activated GB migration, and the metal under consideration is modeled as an elastically isotropic solid. Within the framework of the approach used, we will assume that each of the dislocations that make up the migrating GBs can move only along one slip plane (along the x-axis in Fig. 1b). Such a one-dimensional motion of dislocations is described by the dependencies $x_i(t)$, where x_i is the coordinate of the i-th dislocation ($i = 1,\ldots, N$), and t is the time. Also, we will assume that the dislocations of the migrating boundaries (1) and (2), reaching the high-angle boundaries, are absorbed by them, and thus can no longer move.

To model this one-dimensional motion, it is required to calculate the projection onto the x-axis of the resulting force F_i acting on each dislocation and exerted by the shear stress τ, disclinations at triple junctions, and other dislocations. During the periods of the absence of the applied stress, the movement of dislocations occurs exclusively as a result of their interaction with other defects of the system under consideration. Thus, F_i can be expressed as follows:

$$
\begin{aligned}
F_i = {} & b_i\tau_i + D\sum_{\substack{k=1\\k\neq i}}^{N} b_i b_k \frac{(x_i - x_k)[(x_i - x_k)^2 - (y_i - y_k)^2]}{[(x_i - x_k)^2 + (y_i - y_k)^2]^2} \\
& - Db_i\omega_1\left(\frac{x_i(y_i + L/2)}{x_i^2 + (y_i + L/2)^2} - \frac{x_i(y_i - L/2)}{x_i^2 + (y_i - L/2)^2}\right) \\
& + Db_i\omega_2\left(\frac{(x_i - L)(y_i + L/2)}{(x_i - L)^2 + (y_i + L/2)^2}\right. \\
& \left. - \frac{(x_i - L)(y_i - L/2)}{(x_i - L)^2 + (y_i - L/2)^2}\right),
\end{aligned}
\tag{1}
$$

where $D = G/[2\pi(1-\nu)]$, G is the shear modulus, ν is Poisson's ratio, L is the GB length, (x_i, y_i) are the coordinates of the i-th dislocation. In this case, $b_i = b$, $y_i = h_1(i - 1/2) - L/2$, for $i = 1,\ldots, N_1$, and $b_i = -b$, $y_i = h_2(i - 1/2) - L/2$, for $i = N_1 + 1,\ldots, N_2$, where N_1 and N_2 are the number of dislocations in GBs (1) and (2), respectively $(N_1 + N_2 = N)$. The first term in equation (1) characterizes the force exerted on the i-th dislocation by the resolved shear stress τ_i created by the applied load σ near the crack tip. The second term in equation (1) characterizes the force of the interaction of the i-th dislocation with all the other dislocations of the migrating boundaries (1) and (2). The third and fourth terms characterize the interaction forces of the i-th dislocation with the disclinations at the triple junctions A, B, C, and D.

The resolved shear stress τ_i created by the applied load σ near the crack tip at the position of the i-th dislocation can be calculated by the following formula:

$$
\tau_i = (\sigma_{y_i'y_i'} - \sigma_{x_i'x_i'})\sin\alpha\cos\alpha + \sigma_{x_i'y_i'}\cos 2\alpha, \tag{2}
$$

where $\sigma_{x_i'x_i'}$, $\sigma_{y_i'y_i'}$ and $\sigma_{x_i'y_i'}$ are the components of the stress tensor created by the applied load σ near the crack tip, written in the coordinate system O$x'y'$ with the origin at the point M, which can be represented as [28]:

$$\sigma_{x_i'x_i'} = \frac{K_\mathrm{I}}{\sqrt{2\pi r_i}}\cos(\gamma_i/2)\left[1-\sin(\gamma_i/2)\sin(3\gamma_i/2)\right],$$

$$\sigma_{y_i'y_i'} = \frac{K_\mathrm{I}}{\sqrt{2\pi r_i}}\cos(\gamma_i/2)\left[1+\sin(\gamma_i/2)\sin(3\gamma_i/2)\right]+\sigma,$$

$$\sigma_{x_i'y_i'} = \frac{K_\mathrm{I}}{\sqrt{2\pi r_i}}\sin(\gamma_i/2)\cos(\gamma_i/2)\cos(3\gamma_i/2). \qquad (3)$$

In equations (3) $K_\mathrm{I} = \sigma\sqrt{\pi l}$ is the stress intensity factor and (r_i, γ_i) are the polar coordinates of the i-th dislocation, which can be calculated using the formulas:

$$r_i = \sqrt{x_i'^2 + y_i'^2},$$

$$\gamma_i = \begin{cases} \arctan(y_i'/x_i'), & x_i' > 0, \\ \arctan(y_i'/x_i') + \pi, & x_i' < 0,\ y_i' \geq 0, \\ \arctan(y_i'/x_i') - \pi, & x_i' > 0,\ y_i' < 0, \\ \pi/2, & x_i' = 0,\ y_i' > 0, \\ -\pi/2, & x_i' = 0,\ y_i' < 0, \end{cases} \qquad (4)$$

$$\begin{aligned} x_i' &= (x_i - x_{cr})\cos\alpha - (y_i - y_{cr})\sin\alpha, \\ y_i' &= (x_i - x_{cr})\sin\alpha + (y_i - y_{cr})\cos\alpha, \end{aligned} \qquad (5)$$

where (x_{cr}, y_{cr}) are the coordinates of the point M in the Oxy system.

Within the framework of the used method of two-dimensional dislocation dynamics, the equations of motion of dislocations have the following form:

$$m\frac{d^2x_i}{dt^2} + \beta\frac{dx_i}{dt} = F_i, \quad i = 1,\dots,N, \qquad (6)$$

where $m = \rho b^2/2$ is the dislocation mass [29], ρ is the density of the material, β is the viscosity coefficient.

3. RESULTS

Using equations (1) to (6), the collective migration of two low-angle tilt boundaries stimulated by a periodically acting tensile load in α-Fe was simulated. The following material parameters were used for calculations: $G = 84$ GPa, $\nu = 0.29$, $b = 0.287$ nm, $\rho = 7850$ kg×m^{-3} and $L \approx 98.7$ nm, while β was estimated as 5×10^{-5} Pa×s [30]. Also, the results presented below are given for the values $\omega_1 = 5°$, $\omega_2 = 4.15°$. In the course of the simulation, fixed periods of the action and the absence of an external applied stress were not used, but the migration of dislocations constituting low-angle GBs was considered until they reached high-angle boundaries and/or equilibrium positions. This approach allows us to state that the data obtained are valid for all periods of the presence and absence of σ, equal and greater than those used. The profiles of low-angle GBs during migration were studied at various crack locations (at points G, E and F), crack length l, values of periodically applied stress σ, and misorientation angles θ.

The simulations have shown that during the periods of the presence of the external load, the low-angle GBs approach one another or move away from each other, depending on the level of the applied load σ and the relative position of the crack and the group of grains under consideration (characterized by the angle α). After the disappearance of the applied load, the GBs under consideration tend to return to their initial position.

In our simulations, a number of migration modes were identified at various levels of the applied load σ.

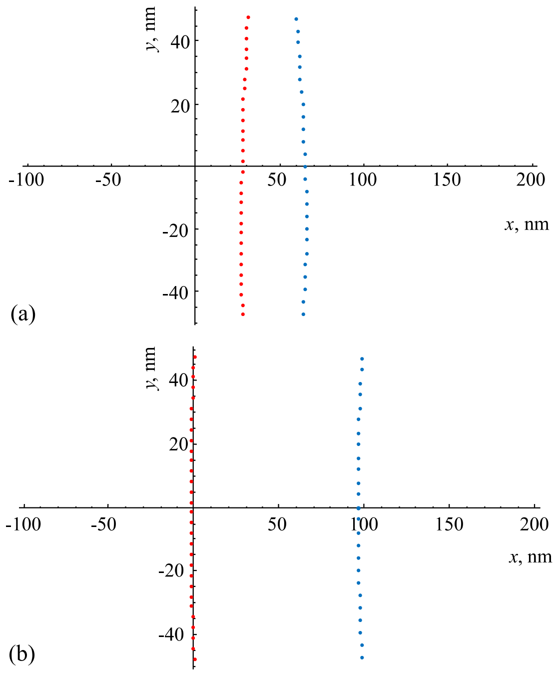

Fig. 2. Characteristic equilibrium profiles of migrating low-angle grain boundaries in the first migration mode. $\alpha = 30°$, $\sigma = 1.4$ GPa, $\mathrm{M}(x,y) = (-L, -L/2)$, $l = 15L$. (a) Equilibrium displacements of migrating GBs under loading. (b) Return of migrating GBs to their initial equilibrium positions. Here and below, the red dots indicate the positions of the dislocations characterized by the Burgers vector **b** (that initially compose the GB AB), and the blue points illustrate the positions of the dislocations characterized by the Burgers vector –**b** (that initially compose the GB CD).

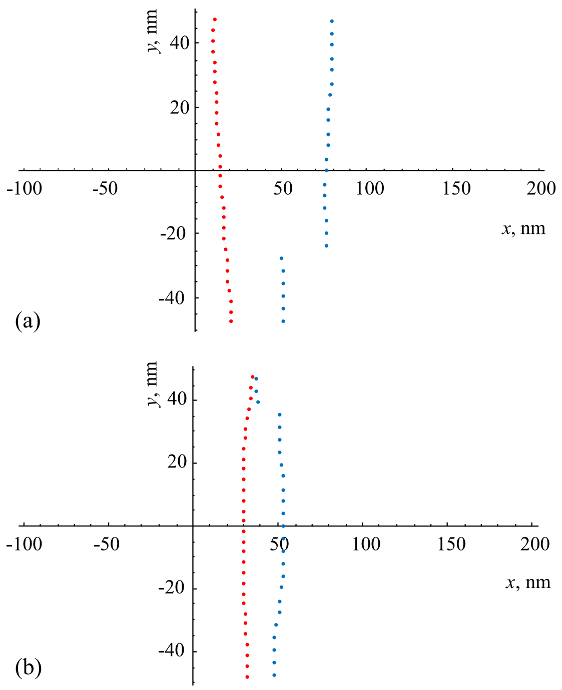

Fig. 3. Characteristic equilibrium profiles of migrating low-angle grain boundaries in the second migration mode. (a) $\alpha = 45°$, $\sigma = 1.6$ GPa, $M(x, y) = (L, L/2)$, $l = 15L$; (b) $\alpha = 30°$, $\sigma = 1.1$ GPa, $M(x, y) = (-L, -L/2)$, $l = 30L$.

In the case of counter migration, at small values of α (less than 5–8°) and physically possible values of σ, the considered GBs remain practically immobile and the average migration of the dislocations of the GBs AB and CD remains within 4 nm. This case can be defined as the first migration mode. With an increase in the angle α and the smallest values of tensile load σ, this mode is fully realized and the GBs under consideration migrate at a considerable distance from their initial positions without reaching each other. In this case, all dislocations of the GBs AB and CD reach their equilibrium positions. In this mode there is an insignificant loss of symmetry of the migrating boundaries relative to the x-axis, which is associated with the influence of the crack. After the disappearance of the load, the migrating GBs tend to return to their initial positions (Fig. 2).

With an increase in the applied load σ, the second migration mode is realized, in which the boundary with a lower misorientation angle is segmented and its part farthest from the crack tip approaches significantly to the GB with a higher misorientation (Fig. 3). In this mode, all dislocations of migrating GBs also reach equilibrium positions and tend to return to their initial positions after the disappearance of the tensile stress. This mode is implemented in a rather narrow range of values of σ and α.

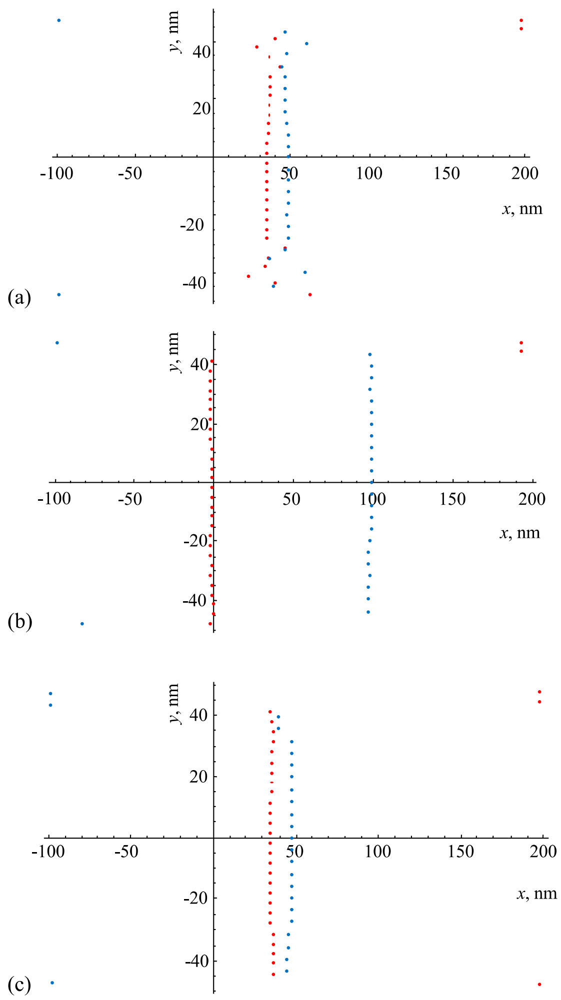

Fig. 4. Characteristic equilibrium profiles of migrating low-angle GBs in the third migration mode. $\sigma = 30°$, $\sigma = 1.9$ GPa, $M(x, y) = (-L, -L/2)$, $l = 15L$. (a) In the first loading cycle, all dislocations reach equilibrium positions or high-angle GBs. (b) During unloading after the first cycle of loading, dislocations not captured by high-angle GBs tend to return to their initial positions. (c) Under a new loading cycle, new dislocations migrate to high-angle GBs.

Fig. 4 shows the GB profiles corresponding to the third migration mode, which manifests itself with a further increase in σ. It is characterized by the gradual passage of some dislocations to high-angle boundaries EF and GH, while the remaining dislocations of migrating GBs reach equilibrium positions. After unloading, the latter tend to return to their initial positions (Fig. 4b). With new loading cycles, more dislocations can travel to high-angle boundaries (Fig. 4c). However, after several loading cycles, the process of capturing new dislocations by high-angle boundaries stops.

With an even greater increase in the applied load σ, migration passes to the fourth mode, in which the

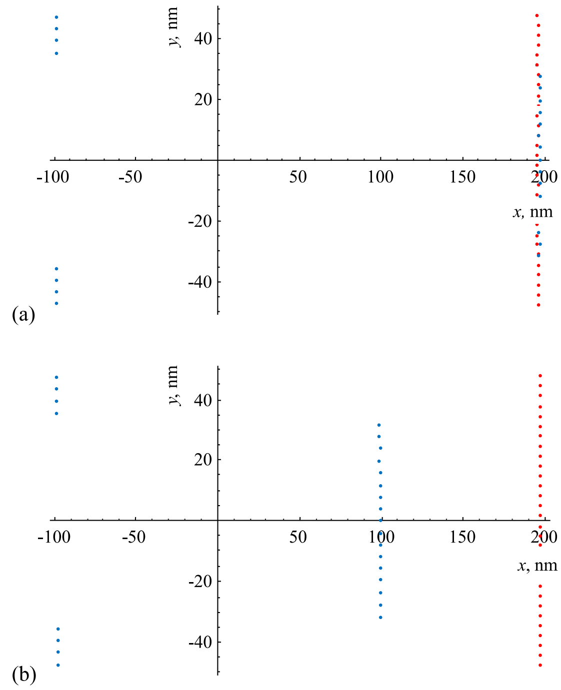

Fig. 5. Characteristic equilibrium profiles of migrating low-angle GBs in the fourth migration mode. $\alpha = 45°$, $\sigma = 2$ GPa, $M(x, y) = (-L, -L/2)$, $l = 30L$. (a) Under loading, low-angle boundaries pass through each other and all dislocations reach equilibrium positions or high-angle GBs, while fragmentation of the GB with a smaller misorientation occurs. (b) During unloading the dislocations of the segment not captured by GBs EF and GH migrate to the nearest high-angle boundary.

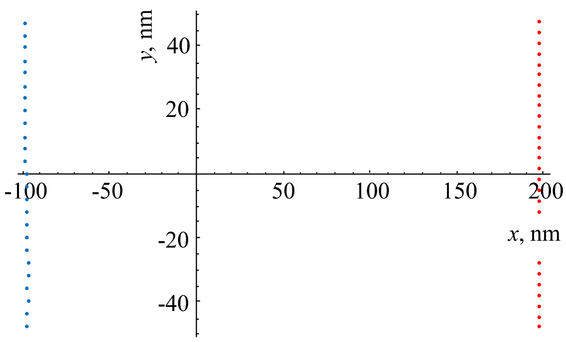

Fig. 6. Characteristic equilibrium profiles of migrating low-angle grain boundaries in the fifth migration mode. $\alpha = 45°$, $\sigma = 2.2$ GPa, $M(x, y) = (-L, -L/2)$, $l = 30L$.

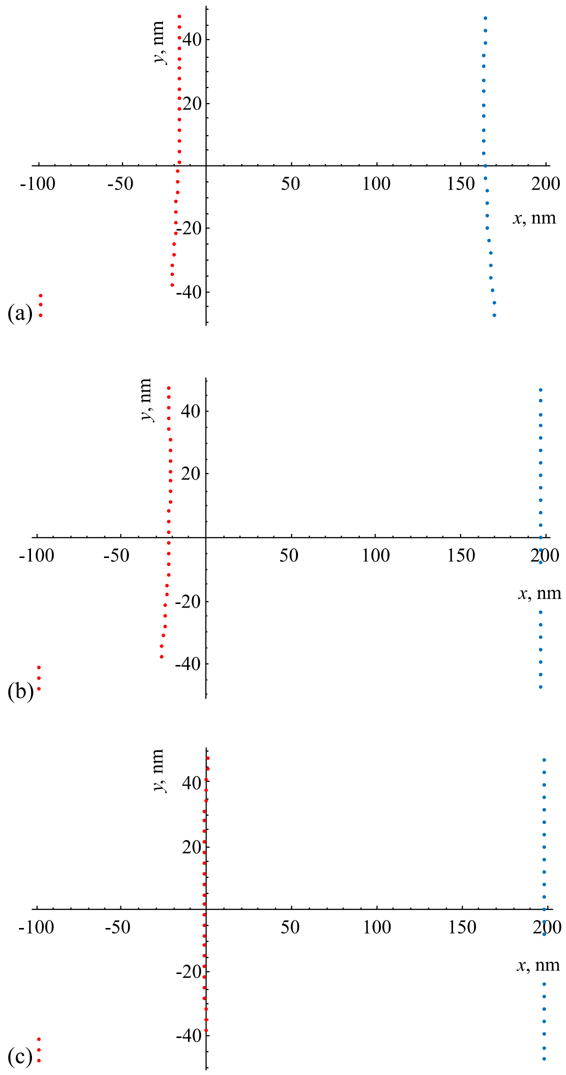

Fig. 7. Characteristic equilibrium profiles of migrating low-angle GBs in the seventh migration mode. (a) $\alpha = -45°$, $\sigma = 1.2$ GPa, $M(x, y) = (-L, -L/2)$, $l = 30L$. Segmentation of closest to the crack migrating GB without capturing of another migrating GB by the high-angle boundary. (b) and (c) $\alpha = -45°$, $\sigma = 1.3$ GPa, $M(x, y) = (-L, -L/2)$, $l = 30L$. Segmentation of the migrating GB, closest to the crack, with capturing of another migrating GB by the high-angle boundary (b). Return of the dislocations not absorbed by high-angle boundaries to the positions close to the initial ones (c).

boundaries AB and CD pass through each other, but the boundary, characterized by a lower misorientation angle θ, is segmented and the dislocations of its central part migrate in the opposite direction, reaching equilibrium positions (Fig. 5a). Other dislocations are captured by high-angle boundaries. After the disappearance of the applied load, the central segment of the GB with a smaller misorientation also migrates to the nearest high-angle boundary (Fig. 5b). Thus, all dislocations of the low-angle GBs under consideration are absorbed by the high-angle boundaries, and the G1, G2, and G3 grains are combined into one.

At the highest values of the applied load σ, a transition to the fifth mode occurs. In this case, the migrating boundaries completely pass through each other and

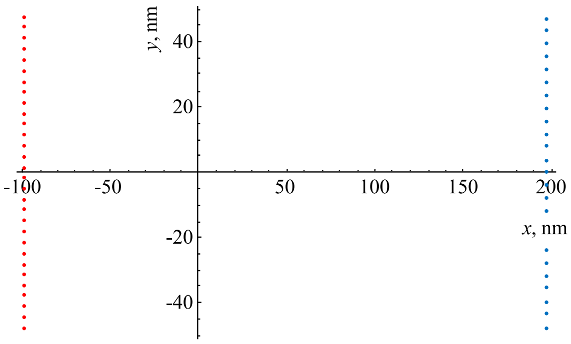

Fig. 8. Characteristic equilibrium profiles of migrating low-angle grain boundaries in the seventh migration mode. $\alpha = 45°$, $\sigma = 1.8$ GPa, $M(x, y) = (-L, -L/2)$, $l = 30L$.

are captured by high-angle GBs (Fig. 6). This mode also corresponds to the coalescence of the considered grains into one.

Now examine the modes of GB migration in the situation where the angle α is negative. In this case, at small absolute values of α and σ, all the GB dislocations that belong to the GBs AB and CD are displaced towards the nearest high-angle boundaries and reach equilibrium positions. After the disappearance of the load, they tend to return to their initial positions before the start of migration (similarly to the first mode). We define this situation as the sixth migration mode.

With an increase in the applied load σ, a transition to the seventh mode is realized, in which the migrating boundary closest to the crack tip is segmented, and its part far from the crack is captured by the high-angle boundary (Fig. 7). In this case, the dislocations of the second low-angle boundary can either reach the high-angle boundary (Fig. 7b) or stop in equilibrium positions (Fig. 7a). After the external load disappears, all "free" dislocations tend to return to their initial positions (Fig. 7c). It should be noted that, under new loading cycles, no increase in the number of the dislocations captured by high-angle boundaries is observed.

At largest values of σ and negative values of α, the eighth migration mode is implemented. In this case, all the dislocations of the GBs AB and CD are captured by the nearest high-angle GBs (Fig. 8). As a result, the considered grains G1-G3 merge.

4. CONCLUSIONS

The method of two-dimensional dislocation dynamics is used to simulate the collective migration of two low-angle GBs in NC metallic materials under the action of a periodically acting tensile load near the crack tip. A number of characteristic modes of migration of low-angle GBs were revealed, which depend on the values of the applied tensile load σ and the angle α that characterizes the positions of the migrating GBs with respect to the crack tip. The results obtained show that the presence of the crack may give rise to specific migration modes. At high enough values of the applied load the collective migration of GBs can lead to grain growth.

REFERENCES

[1] A.K. Mukherjee, *An examination of the constitutive equation for elevated temperature plasticity*, Mater. Sci. Eng. A, 2002, vol. 322, no. 1–2, pp. 1–22. https://doi.org/10.1016/S0921-5093(01)01115-7

[2] I.A. Ovid'ko and T.G. Langdon, *Enhanced ductility of nanocrystalline and ultrafine-grained metals*, Rev. Adv. Mater. Sci., 2012, vol. 30, no. 2, pp. 103–111. https://www.ipme.ru/e-journals/RAMS/no_23012/01_ovidko.pdf

[3] R.Z. Valiev, I. Sabirov, A.P. Zhilyaev and T.G. Langdon, *Bulk nanostructured metals for innovative applications*, JOM, 2012, vol. 64, pp. 1134–1142. https://doi.org/10.1007/s11837-012-0427-9

[4] Y.T. Zhu, X.Z. Liao and X.-L. Wu, *Deformation twinning in nanocrystalline materials*, Prog. Mater. Sci., 2012, vol. 57, pp. 1–62. https://doi.org/10.1016/j.pmatsci.2011.05.001

[5] Y. Estrin and A. Vinogradov, *Extreme grain refinement by severe plastic deformation: A wealth of challenging science*, Acta Mater., 2013, vol. 61, pp. 782–817. https://doi.org/10.1016/j.actamat.2012.10.038

[6] M. Nasim, Y. Li, M. Wen and C. Wen, *A review of high-strength nanolaminates and evaluation of their properties*, J. Mater. Sci., 2020, vol. 50, pp. 215–244. https://doi.org/10.1016/j.jmst.2020.03.011

[7] L.G. Sun, G. Wu, Q. Wang and J. Lu, *Nanostructural metallic materials: Structures and mechanical properties*, Mater. Today, 2020, vol. 38, pp. 114–135. https://doi.org/10.1016/j.mattod.2020.04.005

[8] M.Y. Gutkin and I.A. Ovid'ko, *Grain boundary migration as rotational deformation mode in nanocrystalline materials*, Appl. Phys. Lett., 2005, vol. 87, no. 25, art. no. 251916. https://doi.org/10.1063/1.2147721

[9] M.Yu. Gutkin, K.N. Mikaelyan and I.A. Ovid'ko, *Grain growth and collective migration of grain boundaries during plastic deformation of nanocrystalline materials*, Phys. Solid State, 2008, vol. 50, pp. 1266–1279. https://doi.org/10.1134/S1063783408070135

[10] I.A. Ovid'ko, A.G. Sheinerman and E.C. Aifantis, *Stress-driven migration of grain boundaries and fracture processes in nanocrystalline ceramics and metals*, Acta Mater., 2008, vol. 56, no. 12, pp. 2718–2727. https://doi.org/10.1016/j.actamat.2008.02.004

[11] I.A. Ovid'ko, A.G. Sheinerman and E.C. Aifantis, *Effect of cooperative grain boundary sliding and migration on crack growth in nanocrystalline solids*, Acta Mater., 2011, vol. 59, no. 12, pp. 5023–5031. https://doi.org/10.1016/j.actamat.2011.04.056

[12] S.V. Bobylev and I.A. Ovid'ko, *Stress-driven migration of deformation-distorted grain boundaries in nanomaterials*, Acta Mater., 2015, vol. 88, pp. 260–270. https://doi.org/10.1016/j.actamat.2015.01.052

[13] Y. Lin, H., Wen, Y. Li, B. Wen and E.J. Lavernia, *Stress-induced grain growth in an ultra-fine grained Al alloy*, Metall. Mater. Trans. B, 2014, vol. 45, pp. 795–810. https://doi.org/10.1007/s11663-014-0049-4

[14] Y. Lin, B. Xu, Y. Feng and E.J. Lavernia, *Stress-induced grain growth during high-temperature deformation of nanostructured Al containing nanoscale oxide particles*, J. Alloys Compd., 2014, vol. 596, pp. 79–85. https://doi.org/10.1016/j.jallcom.2014.01.189

[15] K. Dám, P. Lejček and A. Michalcová, *In situ TEM investigation of microstructural behavior of superplastic Al–Mg–Sc alloy*, Mater. Charact., 2013, vol. 76, pp. 69–75. https://doi.org/10.1016/j.matchar.2012.12.005

[16] Y. Lin, H. Wen, Y. Li, B. Wen, L. Wei and E.J. Lavernia, *The role of low-lying optical phonons in lattice thermal conductance of rare-earth pyrochlores: A first-principle study*, Acta Mater., 2015, vol. 82, pp. 304–317. https://doi.org/10.1016/j.actamat.2015.03.004

[17] T. Zálezák and A. Dlouhý, *3D discrete dislocation dynamics applied to interactions between dislocation walls and particles* // Acta Phys. Pol. A, 2012, vol. 122, no. 3, pp. 450–452. http://dx.doi.org/10.12693/APhysPolA.122.450

[18] I.A. Ovid'ko and A.G. Sheinerman, Stress-driven migration of low-angle tilt boundaries in nanocrystalline and ultrafine-grained metals containing coherent nanoinclusions, Rev. Adv. Mat. Sci., 2014, vol. 39, no. 1, pp. 99–107. https://ipme.ru/e-journals/RAMS/no_13914/14_13914_ovidko.pdf

[19] I.A. Ovid'ko and A.G. Sheinerman, *Effects of incoherent nanoinclusions on stress-driven migration of low-angle grain boundaries in nanocomposites*, J. Mater. Sci., 2015, vol. 50, pp. 4430–4439. https://doi.org/10.1007/s10853-015-9011-3

[20] Ya.V. Konakov, I.A. Ovid'ko and A.G. Sheinerman, *Stress-driven migration of low-angle grain boundaries in nanocomposites with incoherent inclusions*, Mater. Phys. Mech., 2015, vol. 24, no. 2, pp. 97–106. https://www.ipme.ru/e-journals/RAMS/no_23012/01_ovidko.pdf

[21] A. Devaraj, W. Wang, R. Vemuri, L. Kovarik, X. Jiang, M. Bowden, J.R. Trelewicz, S. Mathaudhu and A. Rohatgi, *Grain boundary segregation and intermetallic precipitation in coarsening resistant nanocrystalline aluminum alloys*, Acta Mater., 2019, vol. 165, pp. 698–708. https://doi.org/10.1016/j.actamat.2018.09.038

[22] I.A. Ovid'ko, R.Z. Valiev and Y.T. Zhu, *Review on superior strength and enhanced ductility of metallic nanomaterials*, Prog. Mater. Sci., 2018, vol. 94, pp. 462–540. https://doi.org/10.1016/j.pmatsci.2018.02.002

[23] G. Zhou, Q. Huang, Y. Chen, X. Yu and H. Zhou, *Annihilation mechanism of low-angle grain boundary in nanocrystalline metals*, Metals, 2022, vol. 12, no. 3, art. no. 451. https://doi.org/10.3390/met12030451

[24] Ya.V. Konakov, I.A. Ovid'ko, A.G. Sheinerman and N.V. Skiba, *Collective migration of low-angle tilt boundaries in nanocrystalline metals under fatigue loading*, Rev. Adv. Mater. Sci., 2017, vol. 52, no. 1/2, pp. 113–120. https://ipme.ru/e-journals/RAMS/no_15217/15_15217_konakov.pdf

[25] S.V. Bobylev, M.Yu. Gutkin and I.A. Ovid'ko, *Decay of low-angle tilt boundaries in deformed nanocrystalline materials*, J. Phys. D, 2004, vol. 37, no. 2, pp. 269–272. https://doi.org/10.1088/0022-3727/37/2/016

[26] S.V. Bobylev, M.Yu. Gutkin and I.A. Ovid'ko, *Transformations of grain boundaries in deformed nanocrystalline materials*, Acta Mater., 2004, vol. 52, no. 13, pp. 3793–3805. https://doi.org/10.1016/j.actamat.2004.04.029

[27] E.A. Rzhavtsev and M.Yu. Gutkin, *The dynamics of dislocation wall generation in metals and alloys under shock loading*, Scripta Mater., 2015, vol. 100, pp. 102–105. https://doi.org/10.1016/j.scriptamat.2015.01.004

[28] V.V. Panasyuk (ed.), Mechanics of fracture and strength of materials (Naukova Dumka, Kiev, 1988), Vol. 2, P. 17 (in Russian).

[29] U.F. Kocks, A.S. Argon and M.F. Ashby, *Thermodynamics and kinetics of slip*, Prog. Mater. Sci., 1975, vol. 19, pp. 1–291. https://doi.org/10.1016/0079-6425(75)90005-5